JACS
JOURNAL OF THE AMERICAN CHEMICAL SOCIETY
pubs.acs.org/JACS
Article

Insight into the Role of Entropy in Promoting Electrochemical CO_2 Reduction by Imidazolium Cations

Seonmyeong Noh, Yoon Jin Cho, Gong Zhang, and Marcel Schreier*

Cite This: J. Am. Chem. Soc. 2023, 145, 27657−27663
Read Online
ACCESS | Metrics & More | Article Recommendations | Supporting Information

ABSTRACT: The electroreduction of CO_2 plays an important role in achieving a net-zero carbon economy. Imidazolium cations can be used to enhance the rate of CO_2 reduction reactions, but the origin of this promotion remains poorly understood. In this work, we show that in the presence of 1-ethyl-3-methylimidazolium ($EMIM^+$), CO_2 reduction on Ag electrodes occurs with an apparent activation energy near zero, while the applied potential influences the rate through the pre-exponential factor. Our findings suggest that the CO_2 reduction rate is controlled by the initial state entropy, which depends on the applied potential through the organization of cations at the electrochemical interface. Further characterization shows that the C2-proton of $EMIM^+$ is consumed during the reaction, leading to the collapse of the cation organization and a decrease in the catalytic performance. Our results have important implications for understanding the effect of potential on reaction rates, as they indicate that the common picture based on vibrational activation of electron transfer reactions is insufficient for describing the impact of potential in complex systems, such as CO_2 reduction in the presence of imidazolium cations.

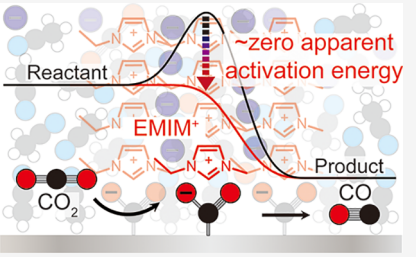

INTRODUCTION

Achieving net-zero carbon emissions requires technologies for the long-term storage of renewable electricity and the sustainable synthesis of chemicals. The electrochemical reduction of CO_2 (CO_2RR) to C1 and C2 carbon feedstocks has the potential to fulfill these needs and has, consequently, received great interest in recent decades.[1−6] Considerable progress has been achieved in understanding the mechanism of CO_2RR.[7−10] Surprisingly, however, the most fundamental question of how the applied potential controls the rate of the CO_2RR has not been conclusively answered. Basic electron transfer models such as the Tafel, Butler−Volmer, and simple Marcus models assume that the applied potential controls reaction rates by modulating the height of the activation barrier (Figure 1a).[11−13] In this picture, ambient heat (k_BT) provides the energy needed to surmount the activation barrier, while the presence of an electrocatalyst and cocatalyst modifies its height.

Since the realization in 2011 that imidazolium (IMIM) cations, specifically 1-ethyl-3-methylimidazolium ($EMIM^+$, **1**), in ionic liquids can significantly reduce the overpotential of CO_2 reduction reactions,[14] the role of imidazolium cations has received considerable attention, with some of the authors of this paper demonstrating the strong correlation between imidazolium cation structure and electrocatalytic potency in 2016.[15] Nevertheless, it remains unclear how imidazolium cations act as cocatalysts at electrochemical interfaces, and multiple mechanisms have been proposed. Some reports suggest that **1** will become reduced at the electrode surface and, subsequently, act as a catalyst that passes electrons on to CO_2 through an inner-sphere reaction (Figure 1b).[16−20] Furthermore, it has been suggested that **1** enhances reaction rates by donating its acidic C2 proton or through a hydrogen-bonding interaction with catalytic surface intermediates.[21] Additionally, some reports have suggested that the C4- and C5-protons on the imidazolium ring are critical to enhancing CO_2RR by stabilizing the transition state leading to a $CO_2^{\bullet-}$ intermediate at the electrode surface.[15,22] Overall, the role of imidazolium cations remains controversial, and rationally tuning them to enhance reaction rates requires deeper mechanistic insight.

Based on the simple theories of electron transfer detailed above, it is commonly assumed that imidazolium cations lower the onset potential of the CO_2RR by lowering the activation barrier. To generate more quantitative insight into this process, we sought to measure the activation energy of CO_2 reduction in the absence and presence of small amounts of two structurally distinct imidazolium cations, **1** and 1-ethyl-2,3-dimethylimidazolium ($EMMIM^+$, **2**, Figure 1c). Our studies, which were carried out under controlled mass transport, shed new light on the kinetics of the CO_2RR in the presence of imidazolium cations. Surprisingly, we find that introducing small amounts of **1** renders the CO_2RR rate independent of temperature but still dependent on the applied potential. This

Received: September 4, 2023
Revised: October 23, 2023
Accepted: October 25, 2023
Published: November 29, 2023

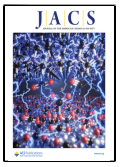

https://doi.org/10.1021/jacs.3c09687
J. Am. Chem. Soc. 2023, 145, 27657−27663

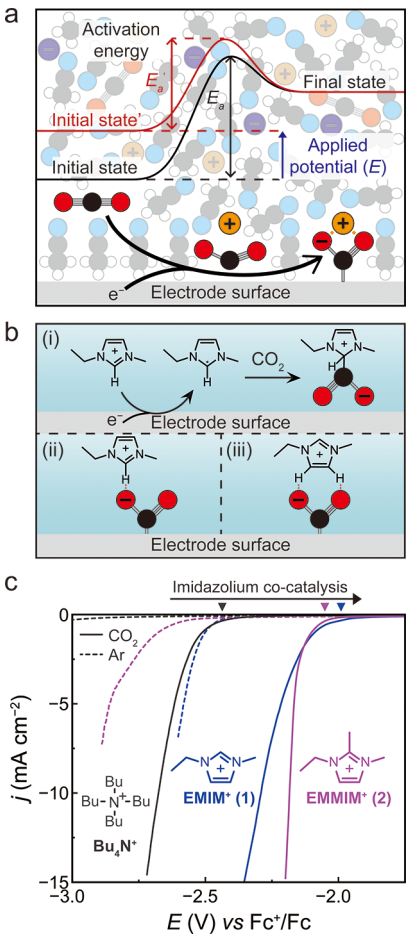

Figure 1. (a) Schematic of the modulation of the CO_2RR by the applied potential. (b) Proposed mechanisms of imidazolium-mediated enhancement of CO_2RR rate (i) Hanc-Scherer et al.[16], (ii) Neyrizi et al.[21], and (iii) Lau, Schreier et al.[15] (c) LSV curves recorded on a Ag electrode under CO_2 (solid line) and Ar (dashed line) for 0.1 M Bu_4NPF_6 electrolytes in MeCN containing no imidazolium cation (dark gray), 50 mM of **1** (blue), and 50 mM of **2** (magenta). Scan rate 100 mV s^{-1}, rotation rate 200 rpm, temperature 20 °C, Pt counter electrode, unseparated cell, *iR*-corrected, and scan in negative direction.

means that in the presence of $EMIM^+$, the CO_2RR exhibits an apparent activation energy near zero. When describing the reaction rate based on the Arrhenius model, the potential impacts the rate primarily through the pre-exponential factor and not through changes to the activation energy. The pre-exponential factor is related to the entropy of activation.[23] In analogy with findings in homogeneous and solution-phase heterogeneous catalysis, we hypothesize that in the presence of imidazolium cations the rate of CO_2RR is controlled by the potential-driven ordering of imidazolium at the electrified interface, which increases the entropy of activation. We further demonstrate that proton abstraction from **1** at higher driving forces produces a neutral species, resulting in the collapse of imidazolium ordering and elimination of the cocatalytic effect. Our results provide novel insight into the mechanism through which applied potentials control reaction rates in electrocatalysis, which we expect to be critical for the development of the electrochemical energy storage and sustainable chemical industries.

RESULTS AND DISCUSSION

To determine the impact of imidazolium cation additives on the CO_2RR performance, we measured the CO_2 reduction rate on Ag electrodes in a CO_2-saturated background electrolyte of 0.1 M Bu_4NPF_6 (Bu_4N^+) in anhydrous acetonitrile (MeCN) (experimental setup shown in Figure S1). The background electrolyte was used to avoid modifying bulk electrolyte conductivity, as the imidazolium additive structure and concentration were changed. Linear sweep voltammetry (LSV) experiments were carried out at 0.1 V s^{-1} on a rotating disc electrode at 200 rpm due to the presence of mass transport effects which we will discuss later. We first measured the rate enhancement due to imidazolium cations by comparing the CO_2RR rate in the presence and absence of 50 mM **1** and **2** (Figure 1c). In the absence of CO_2, the background electrolyte was stable to −3.0 V (all potentials *vs* Fc^+/Fc at the respective temperature), while **1** and **2** underwent irreversible reductive decomposition at −2.45 and −2.55 V, respectively. In the presence of **1** and **2**, we observed a marked lowering of the onset potential compared to the background electrolyte under CO_2, as previously reported.[15,21,22] Compared to **2**, **1** showed a 80 mV earlier onset, but **1** performed worse than **2** as the potential became more negative. We will explain the origin of this effect toward the end of our discussion.

Overall, we found a substantial cocatalytic effect for both **1** and **2** toward CO_2RR on Ag electrodes, which was previously explained by a decrease in the activation energy of CO_2 reduction in the presence of imidazolium cations. To quantify this decrease, we sought to determine the activation energy of the reaction through temperature-dependent measurements of CO_2RR rates in the presence and absence of imidazolium cations.

LSV curves were measured at temperatures ranging from 5 to 35 °C. The Tafel curves determined from these measurements are shown in Figure 2a. Gas chromatography measurements confirmed that the measured current corresponds to the formation of CO (Figure S6). In the pure Bu_4NPF_6 electrolyte, the Tafel curves showed a distinct temperature dependence, with increased temperature resulting in a decreased current at all applied potentials (Figure 2a). In sharp contrast, the presence of **1** resulted in an overlap of the Tafel curves regardless of temperature, indicating that in the presence of imidazolium cation **1**, CO_2RR becomes temperature independent, while remaining dependent on the applied potential. It is generally accepted that in aprotic solvents, CO_2RR is rate limited by the first electron transfer to form a negatively charged CO_2 anion ($CO_2^{\bullet-}$) at the electrode surface.[21] To understand the impact of the temperature on this step and explain our observations, we need to discuss the prevailing models for the rate of electron transfer reactions.

In the simple Tafel model, the rate of a reductive electron transfer is governed by the energy of activation, which is modulated by the potential, relative to the temperature, as shown in eq 1

$$j = -j_{\eta=0} \exp\left(-\frac{\beta e \eta}{k_B T}\right) \quad (1)$$

Here, $\eta = (E - E^0)$ is the overpotential, E is the *iR*-corrected potential (V *vs* Fc^+/Fc), E^0 is the equilibrium potential for CO_2 reduction to CO in MeCN,[24] $j_{\eta=0}$ is the exchange current density, k_B is the Boltzmann constant, T is the temperature, β

https://doi.org/10.1021/jacs.3c09687
J. Am. Chem. Soc. 2023, 145, 27657−27663

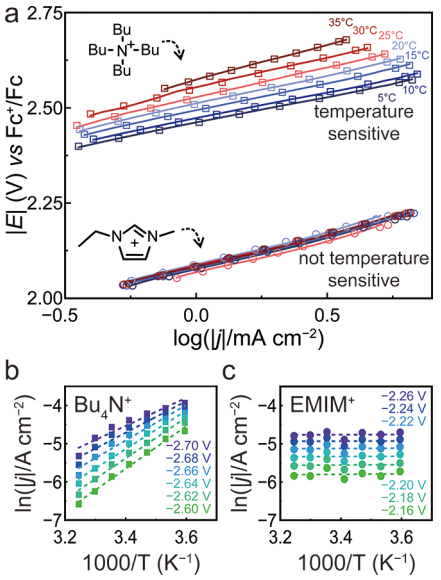

Figure 2. Kinetic investigations of CO_2 reduction electrocatalysis at a Ag electrode at 200 rpm under different temperatures (5−35 °C) and electrolytes. Tafel plots for (a) 0.1 M Bu_4N^+ in MeCN and 50 mM **1** in 0.1 M Bu_4N^+ in MeCN. Corresponding Arrhenius-like plots under various potentials for (b) 0.1 M Bu_4N^+ in MeCN and (c) 50 mM **1** in 0.1 M Bu_4N^+ in MeCN.

is the symmetry factor, and e is the elementary charge (Tables S1−S3). The symmetry factor β expresses how strongly the applied potential changes the activation energy of the reaction, thus modulating the reaction rate at constant temperature. In the simplest interpretation of this model, an increased temperature should lead to an increased reaction rate because more thermal energy is available to overcome the activation barrier. This behavior is not observed in our case and, indeed, we need to refine the model. In 1986, Conway proposed that β should be separated into an enthalpic symmetry factor (β_H) and an entropic symmetry factor (β_S) according to eq 2 (Tables S4−S6).[25,26,28]

$$\beta = \beta_S T + \beta_H \tag{2}$$

This formalism takes into account that the formation of an electron transfer transition state has both an enthalpic and an entropic component, with β_H and β_S representing the impact of the potential on the enthalpy of activation and the entropy of activation, respectively. Interestingly, when fitting our data, in the case of additive **1**, β_H is found to be close to zero, suggesting that the enthalpy of activation exerts a negligible effect on the reaction (Table S5). This becomes obvious when the data are represented in the form of Arrhenius-like plots, where the logarithm of the current density is plotted as a function of $1/T$. The Arrhenius equation describes the rate of a reaction as a function of the activation energy E_a and the pre-exponential factor A (eq 3).

$$k = A\exp\left(\frac{-E_a}{RT}\right) \tag{3}$$

Substituting Faraday's law, a power rate law, and linearizing yields eq 4

$$\ln|j| = \ln(nFc^m A) - \frac{E_a}{RT} \tag{4}$$

where j is the current density, n is the number of electrons transferred, R is the gas constant, c is the CO_2 concentration, and m is the reaction order. It is worth noting that we find the reaction order for CO_2 to be close to zero in the presence of species **1** (Figures S8−S14).

In the case of the pure Bu_4NPF_6 electrolyte in MeCN, we observe a decrease in reaction rate with increasing temperature, pointing to a negative apparent activation energy (Figure S7a). This observation is not uncommon for surface-catalyzed reactions and we suggest that it stems from a decrease in the concentration of dissolved CO_2 (Table S7) and decreased adsorption strength of CO_2 on the catalyst surface at higher temperature.[27,28] In contrast, adding 50 mM of imidazolium **1** results in flat curves of the logarithm of the current density *vs* 1/T, highlighting the temperature independence of the reaction in the presence of **1** and consequently an apparent activation energy near zero (Figure S7b). Based on the Tafel and Butler−Volmer model, E_a is expected to decrease by $\beta_H \eta e$ as η increases in magnitude. However, in the presence of **1**, the apparent activation energy remains near zero regardless of the

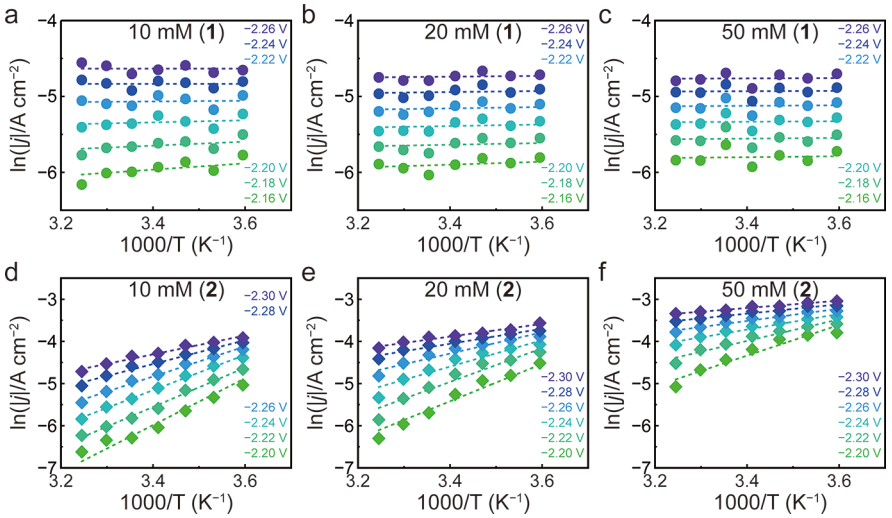

Figure 3. Arrhenius-like plots for CO_2 reduction electrocatalysis at a Ag electrode at 200 rpm in the presence of imidazolium cations with different concentrations at different potentials. (a−c) for **1** in 0.1 M Bu_4N^+ in MeCN; (d−f) for **2** in 0.1 M Bu_4N^+ in MeCN (dashed lines are fits).

https://doi.org/10.1021/jacs.3c09687
J. Am. Chem. Soc. 2023, 145, 27657−27663

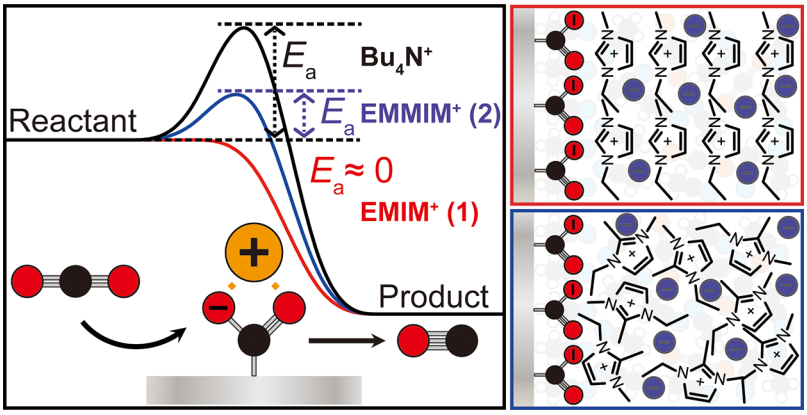

Figure 4. (Left) Schematic illustration of the observed activation enthalpy based on onset potentials and temperature-dependent measurements. (Right) Possible interfacial structure of **1** (top of the right column) and **2** (bottom of the right column). (red circle: oxygen atom; black circle: carbon atom, orange circle: IMIM cation, and navy circle: anions). Illustrations not to scale.

applied potential. In the presence of **1**, the concentration of CO_2 also negligibly impacts the reaction rates. Under these circumstances, the potential controls the reaction rate through the pre-exponential factor A, which is related to the entropy of activation, as expressed by β_S in Conway's theory.

The question thus arises as to why the apparent activation energy of CO_2RR in the presence of **1** is near zero and through what mechanism the potential controls the activation entropy and reaction rate. We propose an explanation based on the structure of the transition state involved in the rate-limiting electron transfer leading to surface-bound $CO_2^{\bullet-}$. Producing this charged intermediate means that formation of the transition state requires recruitment of charge-compensating ions and solvent molecules as described previously, resulting in a lowering of the entropy of the activated complex due to electrostriction.[23] This leads to a negative entropy of activation, $\Delta S^{\ddagger} = S^{\ddagger} - S_i$, where $S^{\ddagger}$ and S_i are the entropy of the activated complex and the initial state, respectively. Since the Gibbs free energy of activation depends on the activation entropy as $\Delta G^{\ddagger} = \Delta H^{\ddagger} - T\Delta S^{\ddagger}$, a more negative entropy of activation will result in a higher free energy of activation and thus a lower reaction rate. Under these circumstances, the lower the entropy of the initial state, i.e., the more ordered the initial state, the lower the entropy of activation. We thus believe that imidazolium cations form an ordered structure at the electrode surface, decreasing the entropy of activation. In this picture, the organization of cations is controlled by their potential-dependent Coulombic attraction to the electrode and should decrease at lower cation concentrations and with ions that possess increased steric bulk. To verify this hypothesis, we measured LSV and Arrhenius data at a lower concentration of **1** (10 and 20 mM, Figures 3, S4, S5, and S7c) and in the presence of the more sterically encumbered imidazolium cation **2**. In both cases, we expected the interfacial cation ordering to be less pronounced. Reducing the concentration of species **1** resulted in a slight decrease in the observed rate and apparent activation energy under low applied bias in agreement with our expectation (Figures 3a and S7b). However, the effect of the cation chemical structure was much more pronounced, with **2** showing a nuanced dependence on cation concentration and applied potential. For all imidazolium concentrations, we observed that the apparent activation energy in the presence of species **2** is negative (Figure S7), which we attribute to the same effects leading to a negative activation energy for Bu_4N^+ as described above. However, the activation energy approaches zero as the applied potential is increased or the temperature is decreased (Figure 3d–f). This trend is amplified under higher concentrations of **2** (Figure 3f). We hypothesize that different imidazolium cations form different structures at the interface, which consequently affect the entropic difference between the initial state and the transition state of CO_2RR. Specifically, we suggest that **1** will form an ordered structure at the interface (low degree of disorganization, reaction controlled by entropic effects),[29] while **2** will feature a more disordered structure, which is less able to stabilize the CO_2 reduction transition state.[30,31] Further evidence for our proposed mechanism comes from the observation that the symmetry factor β for species **1** decreases as the expected degree of ordering increases, supporting the notion that the initial state becomes more similar in nature to the transition state.[25,32,33] CO_2 reduction in the presence of **1** became temperature dependent for 40 °C and above, where more thermal energy is available to promote interfacial disordering, but more strongly so for low concentrations of **1** (Figure S3), reinforcing the idea that interfacial order controls the reaction outcome.

It is worth noting that similar kinetics, featuring near zero-apparent activation energy, have been reported for the liquid-phase hydrogenation of pentacyanocobaltate(II).[34] In that system, the reaction rate was strongly dependent on the ionic strength of the reactant solution, and it was suggested that the rate of reaction is controlled by the formation of a complex ternary transition state involving a hydrogen molecule and two pentacyanocobaltate(II) complexes. It is possible that a similar mechanism is in play for CO_2 reduction in the presence of imidazolium cations, where a transition state is formed that strongly lowers the enthalpy of activation but requires substantial molecular ordering to form. Indeed, it has previously been suggested that the onset of CO_2 reduction in the presence of imidazolium cations is linked to a structural rearrangement.[35] The greater the negative potential, the more aligned and abundant the imidazolium cations are at the interface. In such a case, the more ordered the initial state, the lower the entropic cost of forming the transition state and thus the reaction rate increases (Figure 4). We hypothesize that the methyl group at the C2 position of species **2** introduces steric hindrance which decreases the propensity of the cations to form ordered structures, resulting in a decreased magnitude of the effect observed for species **1**.

https://doi.org/10.1021/jacs.3c09687
J. Am. Chem. Soc. 2023, 145, 27657−27663

When initiating our studies, we realized that CO_2RR in the presence of **1** was mass transfer dependent, as has also been reported by Neyrizi et al.[21] To probe these effects and understand their connection to our hypothesis of structural ordering, we carried out CO_2RR experiments on rotating disc electrodes at multiple rotation rates (Figures 5a,b and S15). In

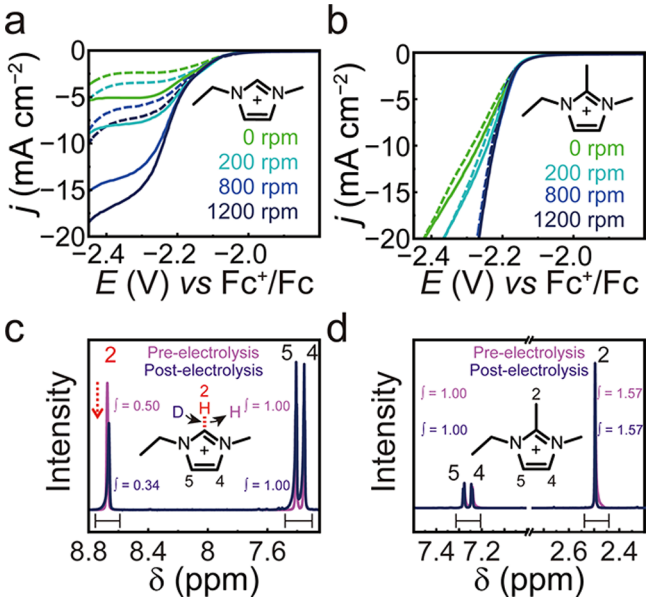

Figure 5. Investigation of the IMIM structural changes during CO_2RR. LSV curves for (a) **1** and (b) **2** at 2 mM concentration (dashed line) and 5 mM concentration (solid line) under a CO_2 atmosphere, recorded at different rotation rates (0−1200 rpm) and at 5 °C. ^{1}H NMR spectra of (c) **1** and (d) **2** acquired before and after CO_2 reduction electrolysis in the presence of 100 mM D_2O. Full spectra in Supporting Information.

the presence of **1**, we observed the appearance of a distinct plateau current at more negative potentials, which depended on the concentration of **1** in solution, as well as on the rotation rate. For species **2**, on the other hand, we did not observe such a plateau, regardless of its concentration in solution. We hypothesized that the plateau is due to the consumption of species **1** during the reaction. **1** possesses an acidic proton at its C2 position, which we theorized to be donated during the reaction. If proton donation occurs, species **1** is reported to form a carbene that is charge neutral and can therefore no longer participate in Coulombic ordering at the electrochemical interface,[36,37] leading to a collapse of the ordered structure and the entropic enhancement. Since **2** does not possess a labile proton at its C2 position, it cannot undergo proton donation and thus remains positively charged at all potentials.

To investigate the viability of our hypothesis, we used nuclear magnetic resonance spectroscopy (^{1}H NMR) to probe the structural changes of species **1** and **2** upon carrying out CO_2 reduction in the presence of D_2O electrolyte (see Supporting Information for detailed ^{1}H NMR spectra, Figures S16−S25 and Tables S8 and S9). Our data showed that the integrated area of the C2-proton (8.69 ppm) decreased by 32% after the reduction of CO_2 in the presence of D_2O (Figure 5c). Such a decrease was not observed in the absence of added D_2O, indicating that the imidazolium cation reversibly regains the donated proton from residual water (Figures S16−S21). No changes in the relative peak integrals before and after CO_2 reduction in the presence of D_2O were observed for species **2** on the other hand, indicating that **2** does not undergo a proton exchange during the reaction (Figures 5d, S22, S23, and S25).

Our observations explain why species **2**, despite having a later onset potential than species **1**, performs better at higher driving force (Figure 1).[15] By donating protons during CO_2 reduction electrolysis, species **1** transforms to a neutral compound, thereby losing its effectiveness in enhancing the reaction rate. This deactivation increases as the current increases up to the observed plateau current. Species **2** is not affected by such a deactivation and therefore exceeds the cocatalytic performance of species **1** at higher currents (Figure S26). We expect future spectroscopic investigations to shed light onto these effects, as prior studies were carried out at potentials and concentrations where loss of ordering would likely not be observed.[35]

CONCLUSIONS

In summary, we investigated the kinetics of the CO_2RR at varying temperatures and in the presence and absence of two distinct imidazolium cations **1** and **2**. We found that the reaction showed no temperature dependence in the presence of **1**, thus exhibiting an apparent activation energy near zero. We attributed this effect to the formation of an ordered structure of imidazolium cations at the electrode surface, which lowers the entropy of activation needed to form the electron transfer transition-state. Even though **1** shows the earliest onset of all cations tested in our study, the collapse of structural ordering due to the donation of the imidazolium C2 proton weakens the enhancement effect of **1**. Our study sheds new light onto the role of applied potential in controlling the rate of electrocatalytic reactions. We expect that our findings on the relationship between interfacial structure and kinetics will contribute to the understanding of the role of cation structure in electrochemical energy storage and sustainable chemical synthesis.

ASSOCIATED CONTENT

Supporting Information

The Supporting Information is available free of charge at https://pubs.acs.org/doi/10.1021/jacs.3c09687.

Detailed experimental methods; photograph of the experimental setup; linear sweep voltammetry; Tafel slopes; quantitative analysis of CO production; enthalpic and entropic symmetry factors; solubility of CO_2 in acetonitrile; apparent activation energy; analysis of kinetics under CO_2 partial pressure; CO_2 reduction reaction order at different temperatures and potentials; isotopic analysis using ^{1}H NMR spectra (PDF)

AUTHOR INFORMATION

Corresponding Author

Marcel Schreier − *Department of Chemical and Biological Engineering, University of Wisconsin−Madison, Madison, Wisconsin 53706, United States; Department of Chemistry, University of Wisconsin−Madison, Madison, Wisconsin 53706, United States;* orcid.org/0000-0002-3674-5667; Email: mschreier2@wisc.edu

Authors

Seonmyeong Noh − *Department of Chemical and Biological Engineering, University of Wisconsin−Madison, Madison, Wisconsin 53706, United States;* orcid.org/0000-0002-2814-5768

Yoon Jin Cho − *Department of Chemical and Biological Engineering, University of Wisconsin−Madison, Madison, Wisconsin 53706, United States;* orcid.org/0009-0005-2999-1199

Gong Zhang − *Department of Chemical and Biological Engineering, University of Wisconsin−Madison, Madison, Wisconsin 53706, United States;* orcid.org/0000-0002-9100-4810

Complete contact information is available at: https://pubs.acs.org/10.1021/jacs.3c09687

Notes

The authors declare no competing financial interest.

■ ACKNOWLEDGMENTS

We acknowledge Megan Kelly for proofreading. This work was supported by a Packard Fellowship for Science and Engineering from the David and Lucile Packard Foundation. We further acknowledge support by the University of Wisconsin−Madison.

■ REFERENCES

(1) Jin, S.; Hao, Z.; Zhang, K.; Yan, Z.; Chen, J. Advances and Challenges for the Electrochemical Reduction of CO_2 to CO: From Fundamentals to Industrialization. *Angew. Chem., Int. Ed.* **2021**, *60*, 20627−20648.

(2) Kibria, M. G.; Edwards, J. P.; Gabardo, C. M.; Dinh, C.-T.; Seifitokaldani, A.; Sinton, D.; Sargent, E. H. Electrochemical CO_2 Reduction into Chemical Feedstocks: From Mechanistic Electrocatalysis Models to System Design. *Adv. Mater.* **2019**, *31*, 1807166.

(3) Wang, G.; Chen, J.; Ding, Y.; Cai, P.; Yi, L.; Li, Y.; Tu, C.; Hou, Y.; Wen, Z.; Dai, L. Electrocatalysis for CO_2 Conversion: from Fundamentals to Value-Added Products. *Chem. Soc. Rev.* **2021**, *50*, 4993−5061.

(4) Li, F.; Thevenon, A.; Rosas-Hernández, A.; Wang, Z.; Li, Y.; Gabardo, C. M.; Ozden, A.; Dinh, C. T.; Li, J.; Wang, Y.; Edwards, J. P.; Xu, Y.; McCallum, C.; Tao, L.; Liang, Z.-Q.; Luo, M.; Wang, X.; Li, H.; O'Brien, C. P.; Tan, C.-S.; Nam, D.-H.; Quintero-Bermudez, R.; Zhuang, T.-T.; Li, Y. C.; Han, Z.; Britt, R. D.; Sinton, D.; Agapie, T.; Peters, J. C.; Sargent, E. H. Molecular Tuning of CO_2-to-Ethylene Conversion. *Nature* **2020**, *577*, 509−513.

(5) Li, L.; Li, X.; Sun, Y.; Xie, Y. Rational Design of Electrocatalytic Carbon Dioxide Reduction for a Zero-carbon Network. *Chem. Soc. Rev.* **2022**, *51*, 1234−1252.

(6) Wu, H.; Singh-Morgan, A.; Qi, K.; Zeng, Z.; Mougel, V.; Voiry, D. Electrocatalyst Microenvironment Engineering for Enhanced Product Selectivity in Carbon Dioxide and Nitrogen Reduction Reactions. *ACS Catal.* **2023**, *13*, 5375−5396.

(7) Zou, Y.; Wang, S. An Investigation of Active Sites for Electrochemical CO_2 Reduction Reactions: From In Situ Characterization to Rational Design. *Adv. Sci.* **2021**, *8*, 2003579.

(8) Martin, D. J.; Mayer, J. M. Oriented Electrostatic Effects on O_2 and CO_2 Reduction by a Polycationic Iron Porphyrin. *J. Am. Chem. Soc.* **2021**, *143*, 11423−11434.

(9) She, X.; Wang, Y.; Xu, H.; Chi Edman Tsang, S.; Ping Lau, S. Challenges and Opportunities in Electrocatalytic CO_2 Reduction to Chemicals and Fuels. *Angew. Chem., Int. Ed.* **2022**, *61*, No. e202211396.

(10) Reid, A. G.; Machan, C. W. Redox Mediators in Homogeneous Co-electrocatalysis. *J. Am. Chem. Soc.* **2023**, *145*, 2013−2027.

(11) Marcus, R. A. Chemical and Electrochemical Electron-Transfer Theory. *Annu. Rev. Phys. Chem.* **1964**, *15*, 155−196.

(12) Marcus, R. A. Electron Transfer Reactions in Chemistry: Theory and Experiment (Nobel Lecture). *Angew. Chem., Int. Ed.* **1993**, *32*, 1111−1121.

(13) Liang, N.; Miller, J. R.; Closs, G. L. Temperature-independent Long-range Electron Transfer Reactions in the Marcus Inverted Region. *J. Am. Chem. Soc.* **1990**, *112*, 5353−5354.

(14) Rosen, B. A.; Salehi-Khojin, A.; Thorson, M. R.; Zhu, W.; Whipple, D. T.; Kenis, P. J. A.; Masel, R. I. Ionic Liquid-Mediated Selective Conversion of CO_2 to CO at Low Overpotentials. *Science* **2011**, *334*, 643−644.

(15) Lau, G. P.; Schreier, M.; Vasilyev, D.; Scopelliti, R.; Gratzel, M.; Dyson, P. J. New Insights into the Role of Imidazolium-Based Promoters for the Electroreduction of CO_2 on a Silver Electrode. *J. Am. Chem. Soc.* **2016**, *138*, 7820−7823.

(16) Hanc-Scherer, F. A.; Montiel, M. A.; Montiel, V.; Herrero, E.; Sánchez-Sánchez, C. M. Surface Structured Platinum Electrodes for the Electrochemical Reduction of Carbon Dioxide in Imidazolium Based Ionic Liquids. *Phys. Chem. Chem. Phys.* **2015**, *17*, 23909−23916.

(17) Kemna, A.; García Rey, N.; Braunschweig, B. Mechanistic Insights on CO_2 Reduction Reactions at Platinum/[BMIM] [BF_4] Interfaces from In Operando Spectroscopy. *ACS Catal.* **2019**, *9*, 6284−6292.

(18) Zhao, S.-F.; Horne, M.; Bond, A. M.; Zhang, J. Is the Imidazolium Cation a Unique Promoter for Electrocatalytic Reduction of Carbon Dioxide? *J. Phys. Chem. C* **2016**, *120*, 23989−24001.

(19) Zhan, T.; Kumar, A.; Sevilla, M.; Sridhar, A.; Zeng, X. Temperature Effects on CO_2 Electroreduction Pathways in an Imidazolium-Based Ionic Liquid on Pt Electrode. *J. Phys. Chem. C* **2020**, *124*, 26094−26105.

(20) Wang, Y.; Hatakeyama, M.; Ogata, K.; Wakabayashi, M.; Jin, F.; Nakamura, S. Activation of CO_2 by ionic liquid EMIM-BF_4 in the electrochemical system: a theoretical study. *Phys. Chem. Chem. Phys.* **2015**, *17*, 23521−23531.

(21) Neyrizi, S.; Kiewiet, J.; Hempenius, M. A.; Mul, G. What It Takes for Imidazolium Cations to Promote Electrochemical Reduction of CO_2. *ACS Energy Lett.* **2022**, *7*, 3439−3446.

(22) Vasilyev, D.; Shirzadi, E.; Rudnev, A. V.; Broekmann, P.; Dyson, P. J. Pyrazolium Ionic Liquid Co-catalysts for the Electroreduction of CO_2. *ACS Appl. Energy Mater.* **2018**, *1*, 5124−5128.

(23) Laidler, K. J. Elementary Reactions in Solution. *Chemical Kinetics*, 3rd ed.; Pearson, 2003; pp 183−228.

(24) Pegis, M. L.; Roberts, J. A. S.; Wasylenko, D. J.; Mader, E. A.; Appel, A. M.; Mayer, J. M. Standard Reduction Potentials for Oxygen and Carbon Dioxide Couples in Acetonitrile and *N*, *N*-Dimethylformamide. *Inorg. Chem.* **2015**, *54*, 11883−11888.

(25) Conway, B. E.; Tessier, D. F.; Wilkinson, D. P. Experimental Evidence for the Potential-Dependence of Entropy of Activation in Electrochemical Reactions in Relations to the Temperature-Dependence of Tafel Slopes. *J. Electroanal. Chem. Interfacial Electrochem.* **1986**, *199*, 249−269.

(26) Conway, B. E.; Wilkinson, D. F. Entropic and Enthalpic Components of the Symmetry Factor for Electrochemical Proton Transfer from Various Proton Donors over a Wide Temperature Range. *J. Electroanal. Chem. Interfacial Electrochem.* **1986**, *214*, 633−653.

(27) Gennaro, A.; Isse, A. A.; Vianello, E. Solubility and Electrochemical Determination of CO_2 in Some Dipolar Aprotic Solvents. *J. Electroanal. Chem. Interfacial Electrochem.* **1990**, *289*, 203−215.

(28) Vos, R. E.; Koper, M. T. M. The Effect of Temperature on the Cation-Promoted Electrochemical CO_2 Reduction on Gold. *ChemElectroChem* **2022**, *9*, No. e202200239.

(29) Rotenberg, B.; Salanne, M. Structural Transitions at Ionic Liquid Interfaces. *J. Phys. Chem. Lett.* **2015**, *6*, 4978−4985.

(30) Devlin, S. W.; Benjamin, I.; Saykally, R. J. On the Mechanisms of Ion Adsorption to Aqueous Interfaces: Air-water vs. Oil-water. *Proc. Natl. Acad. Sci. U.S.A.* **2022**, *119*, No. e2210857119.
(31) Zhang, R.; Han, M.; Ta, K.; Madsen, K. E.; Chen, X.; Zhang, X.; Espinosa-Marzal, R. M.; Gewirth, A. A. Potential-Dependent Layering in the Electrochemical Double Layer of Water-in-Salt Electrolytes. *ACS Appl. Energy Mater.* **2020**, *3*, 8086−8094.
(32) Bockris, J. O. M.; Nagy, Z. Symmetry Factor and Transfer Coefficient. A Source of Confusion in Electrode Kinetics. *J. Chem. Educ.* **1973**, *50*, 839.
(33) Bockris, J. O. M.; Gochev, A. Temperature Dependence of the Symmetry Factor in Electrode Kinetics. *J. Electroanal. Chem. Interfacial Electrochem.* **1986**, *214*, 655−674.
(34) Halpern, J.; Pribanic, M. Hydrogenation of Pentacyanocobaltate(II) at High Pressures. *Inorg. Chem.* **1970**, *9*, 2616−2618.
(35) García Rey, N.; Dlott, D. D. Structural Transition in an Ionic Liquid Controls CO2 Electrochemical Reduction. *J. Phys. Chem. C* **2015**, *119*, 20892−20899.
(36) Amit, E.; Dery, L.; Dery, S.; Kim, S.; Roy, A.; Hu, Q.; Gutkin, V.; Eisenberg, H.; Stein, T.; Mandler, D.; Dean Toste, F.; Gross, E. Electrochemical Deposition of N-Heterocyclic Carbene Monolayers on Metal Surfaces. *Nat. Commun.* **2020**, *11*, 5714.
(37) Gorodetsky, B.; Ramnial, T.; Branda, N. R.; Clyburne, J. A. C. Electrochemical Reduction of an Imidazolium Cation: a Convenient Preparation of Imidazole-2-Ylidenes and Their Observation in an Ionic liquid. *Chem. Commun.* **2004**, 1972−1973.

https://doi.org/10.1021/jacs.3c09687
J. Am. Chem. Soc. 2023, 145, 27657−27663